HIF-1α inhibits ferroptosis and promotes malignant progression in non-small cell lung cancer by activating the Hippo-YAP signalling pathway

SENZHONG ZHENG[1*], JI MO[2*], JING ZHANG[3] and YANG CHEN[1]

Departments of [1]Cardiothoracic Surgery and [2]Respiratory Medicine, Taizhou First People's Hospital, Taizhou, Zhejiang 318020; [3]School of Medical and Pharmaceutical Engineering, Taizhou Vocational and Technical College, Taizhou, Zhejiang 318000, P.R. China

Received July 5, 2022; Accepted January 5, 2023

DOI: 10.3892/ol.2023.13676

Abstract. Ferroptosis and hypoxia-inducible factor 1α (HIF-1α) have critical roles in human tumors. The aim of the present study was to investigate the associations between ferroptosis, HIF-1α and cell growth in non-small cell lung cancer (NSCLC) cells. The lung cancer cell lines SW900 and A549 were evaluated using reverse transcription-quantitative polymerase chain reaction (RT-qPCR) to detect the expression of HIF-1α. Cell Counting Kit-8, flow cytometry and Transwell migration assays were used to measure cell viability, apoptosis and invasion, respectively. The production of reactive oxygen species (ROS) and levels of malondialdehyde (MDA), glutathione (GSH) and ferrous ion (Fe^{2+}) were determined using detection kits. The expression levels of glutathione peroxidase 4 (GPX4) and Yes-associated protein 1 (YAP1) were detected using RT-qPCR and western blotting. The results showed that the expression of HIF-1α was significantly upregulated in NSCLC cells compared with normal human bronchial epithelial cells. Small interfering RNA specific to HIF-1α (si-HIF-1α) significantly decreased the proliferation and invasion of NSCLC cells and increased their apoptosis. si-HIF-1α also increased the levels of ROS, MDA and Fe^{2+} but decreased GSH and GPX4 levels in A549 cells. Additionally, si-HIF-1α increased phosphorylated (p-)YAP1 levels, suppressed GPX4 and YAP1 expression, and attenuated the YAP1 overexpression-induced changes in YAP1, p-YAP1 and GPX4 levels and cell viability. The ferroptosis antagonist ferrostatin-1 partially attenuated the effects of si-HIF-1α on the NSCLC cells, while the ferroptosis agonist erastin further inhibited NSCLC growth by blocking HIF-1α expression. In conclusion, the silencing of HIF-1α induces ferroptosis by suppressing Hippo-YAP pathway activation in NSCLC cells. The present study provides novel insights into the malignant progression of NSCLC and suggests that HIF-1α is an effective target for the treatment of NSCLC.

Correspondence to: Dr Yang Chen, Department of Cardiothoracic Surgery, Taizhou First People's Hospital, 218 Hengjie Road, Taizhou, Zhejiang 318020, P.R. China
E-mail: yangchenchzj@163.com

*Contributed equally

Abbreviations: NSCLC, non-small cell lung cancer; ROS, reactive oxygen species; VEGF, vascular endothelial growth factor; YAP1, Yes-associated protein 1; GPX4, glutathione peroxidase 4; RT-qPCR, reverse transcription-quantitative polymerase chain reaction; CCK-8, Cell Counting Kit-8; OD, optical density; MDA, malondialdehyde; GSH, glutathione

Key words: non-small cell lung cancer, hypoxia-inducible factor 1α, ferroptosis, oxidative stress, Hippo-YAP pathway

Introduction

Non-small cell lung cancer (NSCLC) is the most common type of cancer, accounting for ~85% of all cases of lung cancer, and is a major cause of cancer-associated mortality worldwide (1). In the USA in 2020, there were estimated to be 228,820 new cases of lung cancer and 140,730 new deaths from lung cancer (2). The 5-year survival rate of patients with metastatic NSCLC is estimated to be 6% (3). Despite recent advancements in medical treatment, the 5-year recurrence rate of NSCLC remains high at >20% (4), indicating that it is important to elucidate the molecular mechanisms underlying the progression of NSCLC.

Ferroptosis is an iron-dependent form of oxidative cell death triggered by the accumulation of lethal levels of lipid-based reactive oxygen species (ROS) and lipid peroxidation (5,6). Studies have demonstrated that ferroptosis is critical in tumourigenesis, cancer development and therapy (7-10). For example, ferroptosis is induced in pancreatic cancer cells by artesunate (11), in Huh-7 hepatocellular carcinoma cells by sorafenib (12) and in human gastric cancer cells by erastin (13). Moreover, sorafenib has been reported to induce ferroptosis in NSCLC cells (14).

Hypoxia plays a critical role in tumourigenesis, metastasis and chemotherapy resistance in solid tumours (15-17). The lack of oxygen enhances the expression and stability of hypoxia-inducible factors (HIFs) such as HIF-1α (18). HIF-1α

increases the expression of vascular endothelial growth factor (VEGF) and promotes the proliferation and migration of cancer cells (19). Furthermore, HIF-1α is detectable in 50% of solid tumours with high proliferative characteristics (17,20). Therefore, HIF-1α is a potential target for cancer therapy. Additionally, recent studies have shown that HIF-1α inhibits ferroptosis in hepatocellular carcinoma (21) and gastric cancer (22). However, the association between HIF-1α and ferroptosis during the development of NSCLC remains unclear.

The Hippo-Yes-associated protein (YAP) pathway influences a wide variety of tumour types, including NSCLC (23). YAP1, a transcriptional activator of Hippo signalling, binds to and maintains the stability of HIF-1α protein in the nuclei of tumour cells (24). YAP1 also promotes the proliferation, invasion, migration and chemoresistance of cancer cells (25,26). Wang and Liu (27) found that knockdown of the long non-coding RNA GHET1 inhibited the hypoxia-induced upregulation of HIF-1α expression and nuclear translocation of YAP, thereby reducing the proliferation and invasion of triple-negative breast cancer cells. Furthermore, YAP has been shown to promote ferroptosis in cancer cells including renal cell carcinoma (28), liver cancer (29) and colon cancer (30). Therefore, we hypothesised that HIF-1α blocks ferroptosis in NSCLC by activating the Hippo-YAP pathway.

In the present study, the proliferation, invasion, ferroptosis and oxidative stress levels of NSCLC cells were investigated after the silencing HIF-1α with or without treatment with the ferroptosis antagonist ferrostatin-1 (Fer-1) or ferroptosis agonist erastin. Expression levels of the Hippo-YAP pathway-associated protein YAP1 and ferroptosis marker protein glutathione peroxidase 4 (GPX4) were also detected. HIF-1α and ferroptosis were investigated as a therapeutic target and strategy, respectively, for the treatment of NSCLC.

Materials and methods

Cell culture. SW900 (cat. no. HTB-59) and A549 (cat. no. CRM-CCL-185) human NSCLC and BEAS-2B (cat. no. CRL-9609) human bronchial epithelial cell lines acquired from the American Type Culture Collection were used in the study. The SW900 and A549 cells were maintained in RPMI-1640 (Gibco; Thermo Fisher Scientific, Inc.) supplemented with 4.5 g/l glucose, 4 mmol/l L-glutamine, 10% foetal bovine serum (FBS; Gibco; Thermo Fisher Scientific, Inc.) and 1% penicillin-streptomycin (Gibco; Thermo Fisher Scientific, Inc.). The BEAS-2B cells were cultured in RPMI-1640 containing 10% FBS and 1% penicillin-streptomycin. All cells were cultured in triplicate in 12-well plates ($1x10^5/cm^2$) at 37˚C with 5% CO_2.

Cell transfection. Small interfering RNA (siRNA) specific to HIF-1α (si-HIF-1α, 5'-CGAUGGAAGCACUAGACAAAG-3'), siRNA negative control (si-NC, 5'-CACUGAUUUCAAAUG GUGCUAUU-3') and a sequence for the overexpression (oe) of YAP1 (oe-YAP1; Shanghai GeneChem Co., Ltd.) were cloned into lentiviral vectors (Lenti-Mix: pMDLg/pRRE, pVSV-G, pRSV-Rev; Wuhan GeneCreate Biological Engineering Co., Ltd.). Lentivirus packaging plasmids (50 ng/μl) expressing si-HIF-1α, si-NC, oe-YAP1 and negative control for YAP1 overexpression (oe-NC) were constructed and transfected into SW900 and A549 cells using HighGene transfection reagent (ABclonal Biotech Co., Ltd.) at 37˚C for 72 h. The mRNA expression and protein levels of HIF-1α and YAP1 were confirmed using reverse transcription-quantitative polymerase chain reaction (RT-qPCR) and western blotting, respectively.

Ferroptosis induction or inhibition. To induce ferroptosis, NSCLC cells were treated with 5 μg/ml erastin (Beijing Solarbio Science & Technology Co., Ltd.) for 24 h. Treatment with Fer-1 (10 μmol/l; ABclonal Biotech Co., Ltd.) for 24 h was used to inhibit ferroptosis (7,31). The treatments were performed at 37˚C in the presence of 5% CO_2.

Cell Counting Kit-8 (CCK-8) assay. The proliferation of SW900 and A549 cells was detected using a CCK-8 assay (Beyotime Institute of Biotechnology). Cells (2x10 cells/well) were seeded into 96-well plates (100 μl/well) and cultured for 24, 48, 72 and 96 h. The cells were then incubated with 10 μl CCK-8 solution for 2 h. A microplate reader (Wuxi Hiwell-Diatek Instruments Co., Ltd.) was used to determine the optical density at 450 nm (OD_{450}).

Flow cytometry assay. NSCLC cell apoptosis was detected using an Annexin V-FITC Apoptosis Detection Kit (Beyotime Institute of Biotechnology). In brief, $2x10^5$ cells were resuspended in 500 μl binding buffer and incubated with 5 μl Annexin V-FITC for 30 min at 4˚C in the dark, followed by incubation with 5 μl propidium iodide for 5 min at 25˚C. The apoptosis rate was then detected using flow cytometry with a CytoFLEX S instrument (Beckman Coulter, Inc.) and Cell Quest software (version 5.2.1; BD Biosciences).

Transwell assay. Cell invasion was evaluated using Matrigel-coated Transwell chambers (Corning, Inc.). NSCLC cells ($1x10^6$/ml) were seeded into the upper chambers filled with serum-free RPMI-1640. The lower chambers were filled with complete RPMI-1640, and the cells cultured for 48 h at 37˚C with 5% CO_2. Cells that adhered to the surface of the lower chamber were fixed and stained with 1% crystal violet (Beyotime Institute of Biotechnology) at room temperature for 20 min. Cells were counted in digital photographs captured using a CKX53 microscope (Olympus Corporation).

RNA isolation and RT-qPCR. RNA was isolated from NSCLC and BEAS-2B cells using TRIzol® reagent (Invitrogen; Thermo Fisher Scientific, Inc.). First-strand cDNA was synthesised using a Fastingking gDNA Dispelling RT SuperMix kit (Tiangen Biotech Co., Ltd.) according to the manufacturer's protocol. SYBR Green PCR Master Mix (Xiamen Life Internet Technology Co., Ltd.) and an MX3000P Fast RT-PCR instrument (Agilent Technologies, Inc.) were used for qPCR analysis. The thermocycling conditions were as follows: 95˚C for 3 min; followed by 40 cycles of 95˚C for 12 sec and 62˚C for 40 sec. The expression levels of HIF-1α and YAP1 were determined using the $2^{-\Delta\Delta Cq}$ method (32). GAPDH was used as an internal reference gene. The specific primers used for qPCR analysis were as follows: HIF-1α forward, 5'-AGAGGTTGA GGGACGGAGAT-3' and reverse, 5'-GCACCAAGCAGGTCA TAGGT-3'; YAP1 forward, 5'-TGACCCTCGTTTTGCCAT GA-3' and reverse 5'-GTTGCTGCTGGTTGGAGTTG-3';

GAPDH forward, 5'-GCACCGTCAAGGCTGAGAAC-3' and reverse, 5'-ATGGTGGTGAAGACGCCAGT-3'.

Western blot analysis. Proteins were isolated from NSCLC and BEAS-2B cells using a radioimmunoprecipitation assay lysis buffer (Beyotime Institute of Biotechnology). The isolated protein samples were quantified using a bicinchoninic acid protein assay kit (Beyotime Institute of Biotechnology) and then protein samples (25 μg) were separated using 10% sodium dodecyl sulphate-polyacrylamide gel electrophoresis (Beyotime Institute of Biotechnology). Immunoblotting analysis was performed using polyvinylidene fluoride membranes (Beyotime Institute of Biotechnology). The membranes were blocked with 5% non-fat milk for 6 min at room temperature. For the immunoblotting analysis, the membranes were incubated with specific primary antibodies, namely anti-HIF-1α (1:500; cat. no. ab51608; Abcam), anti-GPX4 (1:5,000; cat. no. ab125066; Abcam), anti-YAP1 (1:5,000; cat. no. ab52771; Abcam), anti-phosphorylated (p)-YAP1 (1:25,000; cat. no. ab76252; Abcam) and anti-GAPDH (1:2,500; cat. no. ab9485; Abcam) antibodies, at 4˚C overnight. Horseradish peroxidase-tagged goat anti-rabbit IgG H&L (1:10,000; cat. no. A0516; Beyotime Institute of Biotechnology) was used as the secondary antibody and incubated with the membranes at room temperature for 1 h. An enhanced chemiluminescence system (Pierce; Thermo Fisher Scientific, Inc.) and automatic digital gel image analysis system (Tanon 3500; Tanon Science & Technology Co., Ltd.) were used to analyse the target proteins.

Enzyme-linked immunosorbent assay. The levels of malondialdehyde (MDA), glutathione (GSH) and ROS in A549 cells were determined using corresponding commercial enzyme-linked immunosorbent assay kits (cat. no. BC0025 for MDA, Beijing Solarbio Science & Technology Co., Ltd.; cat. no. E-BC-K030-M for GSH, Elabscience Biotechnology, Inc.; and cat. no. CA1410 for ROS, Beijing Solarbio Science & Technology Co., Ltd.). A microplate reader was used to measure the OD_{450} value.

Detection of ferrous iron (Fe^{2+}) levels. The concentration of Fe^{2+} in A549 cells was determined using an iron colorimetric assay kit (cat. no. K390-100; BioVision, Inc.). A microplate reader was used to determine the OD_{450} value.

Statistical analysis. All experiments were performed in triplicate. Statistical analyses were conducted using GraphPad Prism 7.0 software (GraphPad Software, Inc.). Experimental data are expressed as the mean ± standard deviation. Differences between two groups were analysed using an unpaired t-test. Differences among three or more experimental groups were analysed using one-way analysis of variance, followed by Tukey's test. $P<0.05$ was considered to indicate a statistically significant difference.

Results

Upregulation of HIF-1α expression in NSCLC cells. The expression levels of HIF-1α in SW900 and A549 NSCLC cell lines and BEAS-2B normal bronchial epithelial cells were detected using RT-qPCR and western blotting. The mRNA and protein expression levels of HIF-1α in the NSCLC cells were significantly higher than those in the normal cells ($P<0.01$). In addition, the mRNA and protein expression levels of HIF-1α in A549 cells were higher than those in SW900 cells ($P<0.05$; Fig. 1A and B). The knockdown of HIF-1α in NSCLC cells by transfection with si-HIF-1α significantly decreased the mRNA and protein expression levels of HIF-1α compared with the respective levels in cells transfected with si-NC ($P<0.01$; Fig. 1C and D).

si-HIF-1α inhibits malignant progression and induces ferroptosis in NSCLC cells. The effects of HIF-1α silencing on the malignant progression of NSCLC were investigated. The CCK-8 assay showed that HIF-1α silencing significantly suppressed the proliferation of SW900 and A549 cells compared with the proliferation in the respective si-NC group ($P<0.05$; Fig. 2A). Additionally, the flow cytometry results showed that the silencing of HIF-1α significantly increased the apoptosis of SW900 and A549 cells ($P<0.01$; Fig. 2B). Moreover, the knockdown of HIF-1α significantly decreased the invasion ability of SW900 and A549 cells compared with that of the SW900 and A549 cells transfected with si-NC ($P<0.01$; Fig. 2C). Based on the aforementioned results, A549 cells were selected for further analysis.

Lipid peroxidation, GSH depletion and iron accumulation are reported to be critical events in ferroptosis (33). To explore whether HIF-1α expression affects ferroptosis in NSCLC, the levels of ROS, MDA, GSH and Fe^{2+} in A549 cells were measured. si-HIF-1α transfection significantly increased the levels of ROS, MDA and Fe^{2+} and decreased the production of GSH in A549 cells, compared with the levels in A549 cells transfected with si-NC ($P<0.01$; Fig. 2D). GPX4 is a key indicator of ferroptosis (34) and has a regulatory relationship with HIF-1α (35). Therefore, the expression of GPX4 in NSCLC cells was evaluated. Western blotting showed that the knockdown of HIF-1α in A549 cells significantly downregulated GPX4 expression compared with that in the si-NC group ($P<0.001$; Fig. 2E).

si-HIF-1α inhibits Hippo-YAP pathway activation in NSCLC cells. The underlying mechanism by which si-HIF-1α induced ferroptosis in NSCLC cells was then investigated. The Hippo-YAP pathway regulates ferroptosis in cancer (36). Thus, cell viability was examined, as well as the expression of the Hippo-YAP pathway regulator YAP1 and ferroptosis marker GPX4 in A549 cells using CCK-8, RT-qPCR and western blotting assays. As shown in Fig. 3A, YAP1 expression in A439 cells was significantly increased following transfection with oe-YAP1 compared with that in cells transfected with oe-NC ($P<0.001$). RT-qPCR analysis showed that suppression of HIF-1α significantly downregulated the mRNA expression of YAP1 ($P<0.05$). Moreover, the silencing of HIF-1α attenuated the oe-YAP1-induced upregulation of YAP1 mRNA expression ($P<0.01$; Fig. 3B). The silencing of HIF-1α also attenuated the increase in cell viability induced by oe-YAP1 transfection ($P<0.01$; Fig. 3C). As shown in Fig. 3D, the p-YAP1/YAP1 ratio was significantly upregulated in the si-HIF-1α group compared with the si-NC group ($P<0.001$). The inhibitory effect of oe-YAP1 on the p-YAP1/YAP1 ratio was significantly

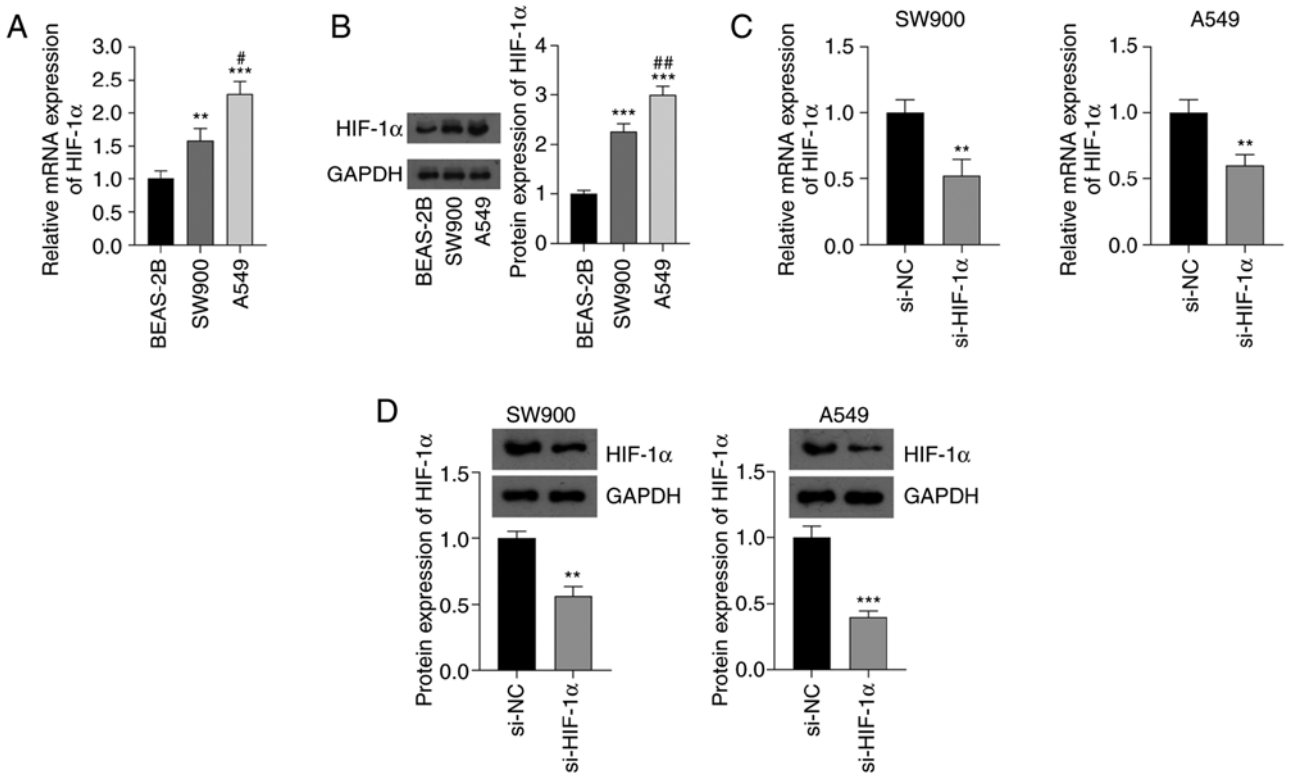

Figure 1. Expression of HIF-1α in NSCLC cells. (A) Expression of HIF-1α mRNA in SW900 and A549 NSCLC cell lines and normal BEAS-2B cells determined using reverse transcription-quantitative polymerase chain reaction. (B) Results of the western blot analysis of HIF-1α protein. In (A) and (B), **P<0.01 and ***P<0.001 vs. BEAS-2B; and $^{\#}$P<0.05 and $^{\#\#}$P<0.01 vs. SW900. (C) mRNA and (D) protein expression of HIF-1α in NSCLC cells transfected with si-HIF-1α. In (C) and (D), **P<0.01 and ***P<0.001 vs. si-NC. HIF-1α, hypoxia-inducible factor 1α; NSCLC, non-small cell lung cancer; si-HIF-1α, small interfering RNA to HIF-1α; si-NC, small interfering RNA negative control.

attenuated by HIF-1α silencing (P<0.001). Furthermore, si-HIF-1α transfection significantly suppressed GPX4 expression compared with that in the si-NC group (P<0.001), and the increase in GPX4 expression induced by YAP1 overexpression was significantly weakened by HIF-1α silencing (P<0.01).

si-HIF-1α promotes ferroptosis by inhibiting Hippo-YAP pathway activation in NSCLC cells. To confirm that si-HIF-1α-induced ferroptosis plays an important role in NSCLC treatment, the proliferation and invasion of A549 cells, and the oxidative stress and iron accumulation in these were cells investigated after treatment with Fer-1 or erastin. As shown in Fig. 4A-C, Fer-1 significantly attenuated the inhibition of cell viability and invasion in A549 cells induced by si-HIF-1α; by contrast, erastin treatment augmented the si-HIF-1α-induced suppression of A549 cell proliferation and invasion (P<0.05). The enzyme-linked immunosorbent assay results indicated that Fer-1 significantly inhibited the si-HIF-1α-induced production of ROS, MDA and Fe^{2+} and reduction in GSH levels in A549 cells (P<0.01; Fig. 4D). By contrast, erastin treatment increased the production of ROS, MDA and Fe^{2+} and further reduced GSH levels in si-HIF-1α-transfected A549 cells (P<0.01; Fig. 4D). Additionally, RT-qPCR and western blot analyses showed that Fer-1 and erastin treatment did not alter the HIF-1α mRNA and protein levels of the A549 cells. However, Fer-1 significantly increased the levels of YAP1 mRNA and GPX4 protein and decreased the p-YAP1/YAP1 ratio compared with those in the si-HIF-1α group (P<0.05), while erastin augmented the si-HIF-1α-induced downregulation of YAP1 mRNA and GPX4 protein expression and upregulation of the p-YAP1/YAP1 ratio (P<0.01; Fig. 4E and F).

Discussion

In recent years, ferroptosis has emerged as a strategy for cancer treatment. The present study evaluated the ability of HIF-1α silencing to induce ferroptosis in NSCLC cells and investigated whether the underlying mechanism involves the inhibition of Hippo-YAP pathway activation.

Hypoxia is a common condition in the tumour environment due to the high proliferation rate of tumour cells (37-39). HIF-1α is an oncoprotein induced by intratumoural hypoxia (40), which promotes tumour cell proliferation, metastasis and migration (15-17,39). VEGF is a key contributor to angiogenesis, and the inhibition of HIF-1α has been shown to decrease VEGF expression in malignant glioma cells and reduce tumour growth (41). The present study confirmed that HIF-1α is upregulated in NSCLC cells compared with normal bronchial epithelial cells. Furthermore, the inhibition of HIF-1α significantly decreased the proliferation and invasion of NSCLC cells and increased their apoptosis. Therefore, the inhibition of HIF-1α shows potential as a mechanism for NSCLC therapy.

As HIF-1α contributes to the inhibition of ferroptosis in hepatocellular carcinoma, it has been reported as a potential

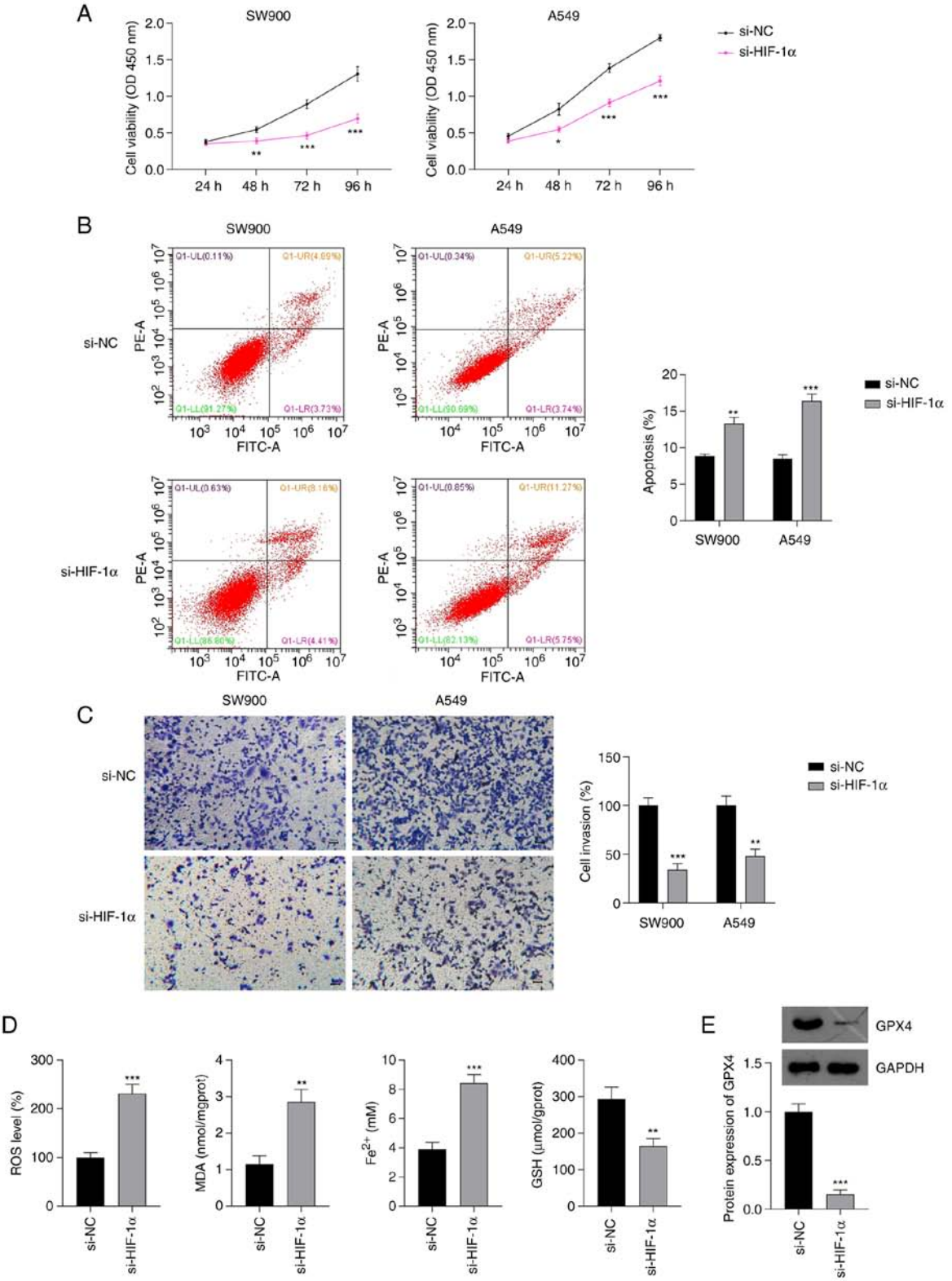

Figure 2. Effect of si-HIF-1α on the proliferation, invasion and ferroptosis of NSCLC cells. Results of (A) Cell Counting Kit-8, (B) flow cytometry and (C) Transwell invasion assays of NSCLC cells transfected with si-HIF-1α. (D) Levels of ROS, MDA, Fe^{2+} and GSH in A549 cells transfected with si-HIF-1α. Scale bar, 50 μm. (E) Protein expression of GPX4 in A549 cells transfected with si-HIF-1α. *P<0.05, **P<0.01 and ***P<0.001 vs. si-NC. si-HIF-1α, small interfering RNA to hypoxia-inducible factor 1α; NSCLC, non-small cell lung cancer; ROS, reactive oxygen species; MDA, malondialdehyde; Fe^{2+}, ferrous iron; GSH, glutathione; GPX4, glutathione peroxidase 4; si-NC, small interfering RNA negative control; OD, optical density.

biomarker of poor post-operative outcomes in this disease (21). Ferroptosis is a form of iron-dependent, non-apoptotic cell death induced by lipid peroxidation, system x_c^- inhibitors and ROS accumulation (42,43). Hypoxia accelerates lipid peroxidation, depletes intracellular GSH (44) and prevents ferroptosis (45,46). These activities were evaluated in the present study following the knockdown of HIF-1α. The results revealed that HIF-1α knockdown significantly increased the

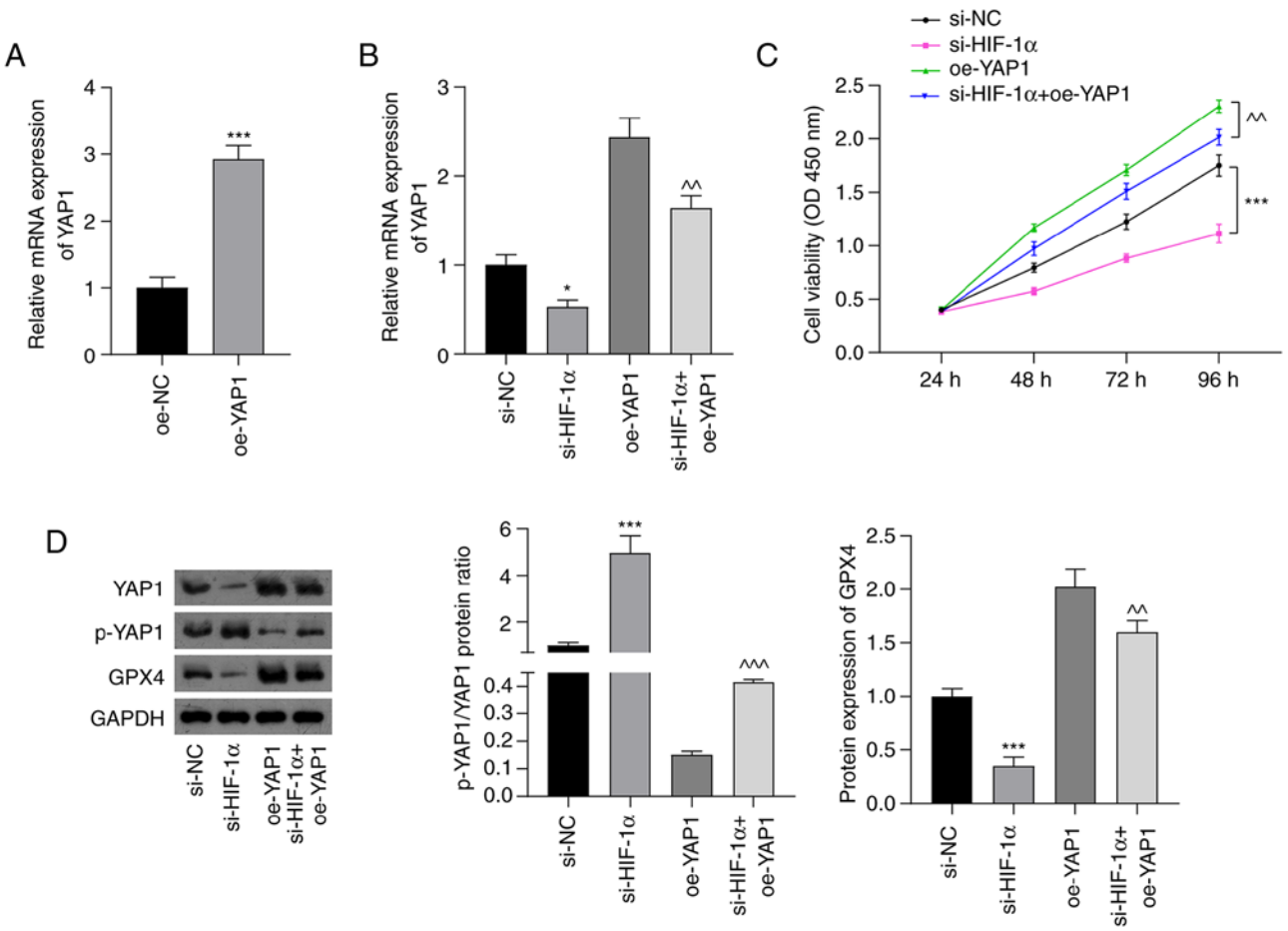

Figure 3. si-HIF-1α inhibits Hippo-YAP pathway activation in non-small cell lung cancer cells. (A) Relative mRNA expression of YAP1 in A549 cells transfected with oe-NC and oe-YAP1. ***P<0.001 vs. oe-NC. (B) Relative expression of YAP1 mRNA in cells transfected with si-HIF-1α and/or oe-YAP1. (C) Cell Counting Kit-8 assay results showing the viability of A549 cells. (D) Fold-change in the p-YAP1/YAP1 ratio and GPX4 protein expression assessed using western blot analysis. *P<0.05 and ***P<0.001 vs. si-NC; ^^P<0.01 and ^^^P<0.001 vs. oe-YAP1. si-HIF-1α, small interfering RNA to hypoxia-inducible factor 1 α; YAP, Yes-associated protein; p-, phosphorylated; oe-YAP1, overexpression of YAP1; oe-NC, overexpression negative control; si-NC, small interfering RNA negative control; GPX4, glutathione peroxidase 4; OD, optical density.

ROS, MDA and Fe^{2+} levels and decreased the GSH levels of NSCLC cells, suggesting that HIF-1α silencing facilitates the ferroptosis of these cells. Further, GPX4 is a prominent regulator of ferroptosis in cancer cells, and GSH depletion has been demonstrated to induce GPX4 inactivation and ferroptosis (34). Additionally, other studies have shown that the inhibition GPX4 leads to lipid peroxidation and ferroptosis (42,47,48). The present study showed that the transfection of NSCLC cells with si-HIF-1α downregulated GPX4 expression, which is consistent with the findings of previous research (35). In addition, the effects of Fer-1 and erastin, which are classical antagonists and agonists of ferroptosis, respectively were investigated. Fer-1 reversed the effects of si-HIF-1α on proliferation, invasion, ROS production, and Fe^{2+} and GPX4 levels in NSCLC cells, whereas erastin enhanced these effects. These results support the hypothesis that HIF-1α silencing inhibits malignant progression by promoting ferroptosis in NSCLC cells.

The Hippo signalling pathway has tumour suppressing effects, and YAP acts as an oncogene in most tumour cells (24,49). Hypoxia promotes the nuclear localisation of YAP and decreases the phosphorylation of YAP in cancer cells (24). In addition, YAP promotes the proliferation and chemoresistance of cancer cells (26,50,51), and also contributes to the invasion and migration of NSCLC cells (26). A previous study has shown that hypoxia enhances the binding of YAP to HIF-1α in the nucleus and maintains the stability of HIF-1α protein (24). The results of the present study showed that transfection with si-HIF-1α decreased the expression of YAP1 in NSCLC cells, and attenuated the oe-YAP1-induced changes in YAP1 and p-YAP1 levels, suggesting that the silencing of HIF-1α inhibits activation of the Hippo-YAP pathway. Furthermore, the upregulation of GPX4 induced by oe-YAP1 was attenuated by HIF-1α silencing. These results indicate that the silencing of HIF-1α promotes ferroptosis by suppressing Hippo-YAP signalling pathway activation.

The present study had some limitations. First, the pathological mechanisms affecting the growth of cancer cells are complex, and ferroptosis is only one such mechanism; the other mechanisms that may be involved were not evaluated. Second, HIF-1α affects NSCLC cell ferroptosis and may be involved in multiple pathways in addition to the Hippo-YAP pathway. Finally, additional experimental data obtained from techniques such as confocal microscopy or fluorescent probe analyses are required to confirm the results.

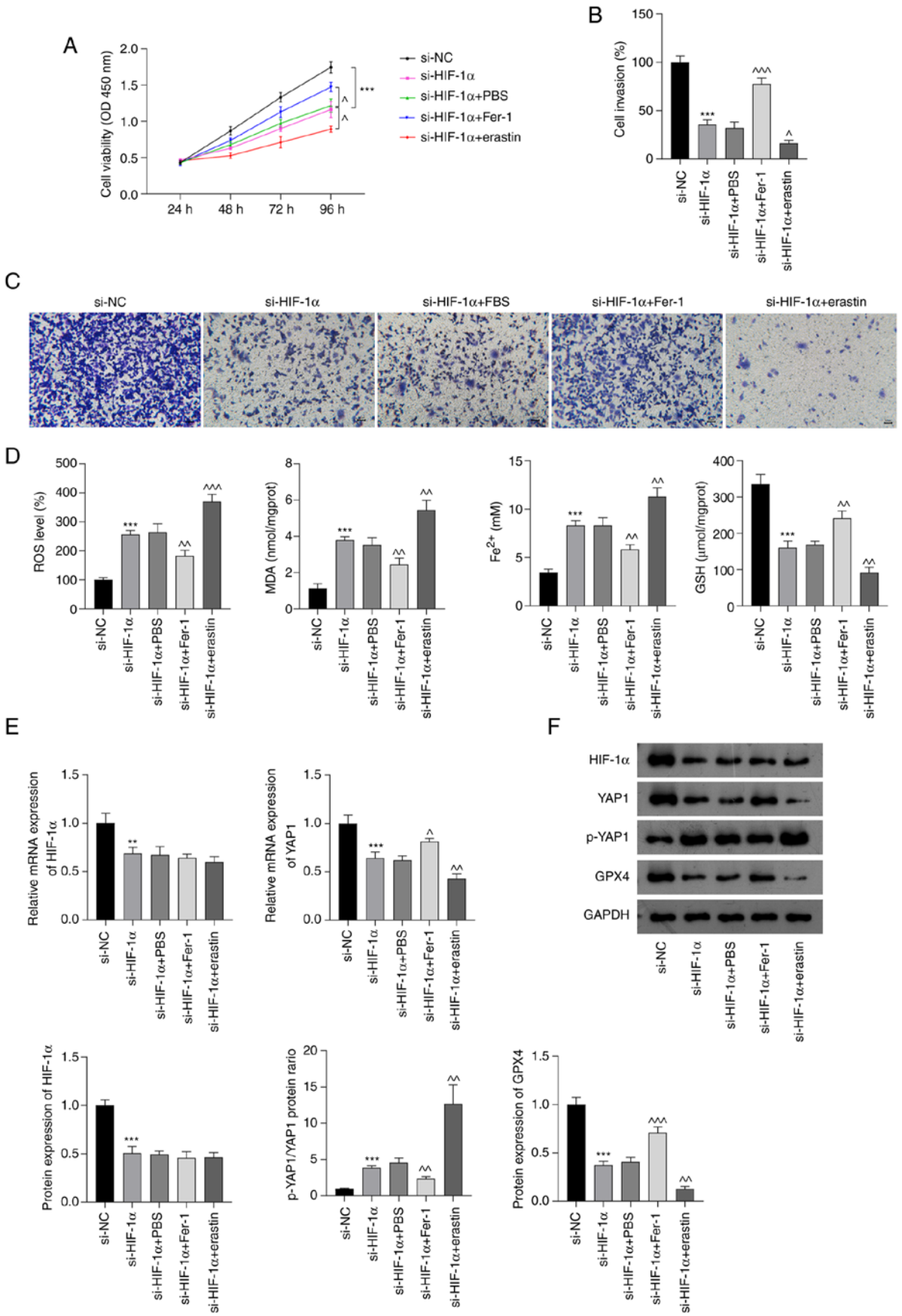

Figure 4. si-HIF-1α promotes ferroptosis by inhibiting Hippo-YAP pathway activation in non-small cell lung cancer cells. (A) Cell Counting Kit-8 assay results. (B) Quantified Transwell invasion assay results and (C) representative images of invaded A549 cells. Scale bar, 50 μm. (D) ROS, MDA, Fe^{2+} and GSH levels in A549 cells. (E) Relative mRNA expression of HIF-1α and YAP1 in A549 cells. (F) Protein levels of HIF-1α, p-YAP1/YAP1 and GPX4 in A549 cells. **P<0.01 and ***P<0.001 vs. si-NC. $^{\wedge}$P<0.05, $^{\wedge\wedge}$P<0.01 and $^{\wedge\wedge\wedge}$P<0.001 vs. si-HIF-1α. HIF-1α, hypoxia-inducible factor 1 α; si-HIF-1α, small interfering RNA to HIF-1α; YAP, Yes-associated protein; p-, phosphorylated; ROS, reactive oxygen species; MDA, malondialdehyde; Fe^{2+}, ferrous iron; GSH, glutathione; GPX4, glutathione peroxidase 4; PBS, phosphate-buffered saline; Fer-1, ferrostatin-1; si-NC, small interfering RNA negative control; OD, optical density.

In conclusion, HIF-1α expression is upregulated in NSCLC cells. The silencing of HIF-1α inhibited the proliferation and invasion of NSCLC cells and induced their ferroptosis; it also suppressed activation of the Hippo-YAP pathway. Moreover, erastin further enhanced the effect of si-HIF-1α whereas Fer-1 counteracted the effect of si-HIF-1α. These results suggest that HIF-1α silencing promotes ferroptosis in NSCLC cells via the inhibition of Hippo-YAP pathway activation. Therefore, HIF-1α is a potential target for NSCLC therapy.

Acknowledgements

Not applicable.

Funding

This study was supported by the Project of Taizhou Science and Technology Bureau (grant no. 21ywb51).

Availability of data and materials

The datasets used and/or analyzed during the current study are available from the corresponding author on reasonable request.

Authors' contributions

SZ, JM and YC contributed to the conception and the design of the study. SZ, JM and JZ were responsible for the acquisition, analysis and interpretation of the data. SZ, JZ and YC confirm the authenticity of all the raw data. SZ and JM contributed to manuscript drafting and critical revisions of intellectual content. SZ obtained the funding. YC approved the final manuscript for publication. All authors have read and approved the final version of the manuscript.

Ethics approval and consent to participate

Not applicable.

Patient consent for publication

Not applicable.

Competing interests

The authors declare that they have no competing interests.

References

1. Fashoyin-Aje LA, Fernandes LL, Sridhara R, Keegan P and Pazdur R: Demographic composition of lung cancer trials: FDA analysis. J Clin Oncol 36 (15_suppl): S9088, 2018.
2. Siegel RL, Miller KD and Jemal A: Cancer statistics, 2020. CA Cancer J Clin 70: 7-30, 2020.
3. Salgia R, Pharaon R, Mambetsariev I, Nam A and Sattler M: The improbable targeted therapy: KRAS as an emerging target in non-small cell lung cancer (NSCLC). Cell Rep Med 2: 100186, 2021.
4. Goodgame B, Viswanathan A, Zoole J, Gao F, Miller CR, Subramanian J, Meyers BF, Patterson AG and Govindan R: Risk of recurrence of resected stage I non-small cell lung cancer in elderly patients as compared with younger patients. J Thorac Oncol 4: 1370-1374, 2009.
5. Dixon SJ, Lemberg KM, Lamprecht MR, Skouta R, Zaitsev EM, Gleason CE, Patel DN, Bauer AJ, Cantley AM, Yang WS, *et al*: Ferroptosis: An iron-dependent form of nonapoptotic cell death. Cell 149: 1060-1072, 2021.
6. Imai H, Matsuoka M, Kumagai T, Sakamoto T and Koumura T: Lipid peroxidation-dependent cell death regulated by GPx4 and ferroptosis. Curr Top Microbiol Immunol 403: 143-170, 2017.
7. Tang X, Ding H, Liang M, Chen X, Yan Y, Wan N, Chen Q, Zhang J and Cao J: Curcumin induces ferroptosis in non-small-cell lung cancer via activating autophagy. Thoracic Cancer 12: 1219-1230, 2021.
8. Nie J, Lin B, Zhou M, Wu L and Zheng T: Role of ferroptosis in hepatocellular carcinoma. J Cancer Res Clin Oncol 144: 2329-2337, 2018.
9. Liang C, Zhang X, Yang M and Dong X: Recent progress in ferroptosis inducers for cancer therapy. Adv Mater 31: e1904197, 2019.
10. Shen Z, Song J, Yung BC, Zhou Z, Wu A and Chen X: Emerging strategies of cancer therapy based on ferroptosis. Adv Mater 30: e1704007, 2018.
11. Eling N, Reuter L, Hazin J, Hamacher-Brady A and Brady NR: Identification of artesunate as a specific activator of ferroptosis in pancreatic cancer cells. Oncoscience 2: 517-532, 2015.
12. Li ZJ, Dai HQ, Huang XW, Feng J, Deng JH, Wang ZX, Yang XM, Liu YJ, Wu Y, Chen PH, *et al*: Artesunate synergizes with sorafenib to induce ferroptosis in hepatocellular carcinoma. Acta Pharmacol Sin 42: 301-310, 2021.
13. Hao S, Yu J, He W, Huang Q, Zhao Y, Liang B, Zhang S, Wen Z, Dong S, Rao J, *et al*: Cysteine dioxygenase 1 mediates erastin-induced ferroptosis in human gastric cancer cells. Neoplasia 19: 1022-1032, 2017.
14. Li Y, Yan H, Xu X, Liu H, Wu C and Zhao L: Erastin/sorafenib induces cisplatin-resistant non-small cell lung cancer cell ferroptosis through inhibition of the Nrf2/xCT pathway. Oncol Lett 19: 323-333, 2020.
15. Li H, Jia Y and Wang Y: Targeting HIF-1α signaling pathway for gastric cancer treatment. Pharmazie 74: 3-7, 2019.
16. Qin Y, Liu HJ, Li M, Zhai DH, Tang YH, Yang L, Qiao KL, Yang JH, Zhong WL, Zhang Q, *et al*: Salidroside improves the hypoxic tumor microenvironment and reverses the drug resistance of platinum drugs via HIF-1α signaling pathway. EBioMedicine 38: 25-36, 2018.
17. Pezzuto A and Carico E: Role of HIF-1 in cancer progression: Novel insights. A review. Curr Mol Med 18: 343-351, 2018.
18. Park SY, Jeong KJ, Lee J, Yoon DS, Choi WS, Kim YK, Han JW, Kim YM, Kim BK and Lee HY: Hypoxia enhances LPA-induced HIF-1alpha and VEGF expression: Their inhibition by resveratrol. Cancer Lett 258: 63-69, 2007.
19. Kim DH, Sung B, Kang YJ, Hwang SY, Kim MJ, Yoon JH, Im E and Kim ND: Sulforaphane inhibits hypoxia-induced HIF-1α and VEGF expression and migration of human colon cancer cells. Int J Oncol 47: 2226-2232, 2015.
20. Ma Z, Xiang X, Li S, Xie P, Gong Q, Goh BC and Wang L: Targeting hypoxia-inducible factor-1, for cancer treatment: Recent advances in developing small-molecule inhibitors from natural compounds. Semin Cancer Biol 80: 379-390, 2022.
21. Zhao J, Zeng G, Lin E, Cai C, Li P, Zou B and Li J: Combined HIF-1α and SHH Up-Regulation Is a Potential Biomarker to Predict Poor Prognosis in Postoperative Hepatocellular Carcinoma. J Invest Surg 35: 1660-1667, 2022.
22. Lin Z, Song J, Gao Y, Huang S, Dou R, Zhong P, Huang G, Han L, Zheng J, Zhang X, *et al*: Hypoxia-induced HIF-1α/lncRNA-PMAN inhibits ferroptosis by promoting the cytoplasmic translocation of ELAVL1 in peritoneal dissemination from gastric cancer. Redox Biol 52: 102312, 2022.
23. Zhang G, Dai S, Chen Y, Wang H, Chen T, Shu Q, Chen S, Shou L and Cai X: Aqueous extract of Taxus chinensis var. mairei regulates the Hippo-YAP pathway and promotes apoptosis of non-small cell lung cancer via ATF3 in vivo and in vitro. Biomed Pharmacother 138: 111506, 2021.
24. Zhang X, Li Y, Ma Y, Yang L, Wang T, Meng X, Zong Z, Sun X, Hua X and Li H: Yes-associated protein (YAP) binds to HIF-1α and sustains HIF-1α protein stability to promote hepatocellular carcinoma cell glycolysis under hypoxic stress. J Exp Clin Cancer Res 37: 216, 2018.
25. Li C, Wang S, Xing Z, Lin A, Liang K, Song J, Hu Q, Yao J, Chen Z, Park PK, *et al*: A ROR1-HER3-lncRNA signalling axis modulates the Hippo-YAP pathway to regulate bone metastasis. Nat Cell Biol 19: 106-119, 2017.

26. Yu M, Chen Y, Li X, Yang R, Zhang L, Huangfu L, Zheng N, Zhao X, Lv L, Hong Y, *et al*: YAP1 contributes to NSCLC invasion and migration by promoting Slug transcription via the transcription co-factor TEAD. Cell Death Dis 9: 464, 2018.
27. Wang Y and Liu S: LncRNA GHET1 promotes hypoxia-induced glycolysis, proliferation, and invasion in triple-negative breast cancer through the Hippo/YAP signaling pathway. Front Cell Dev Biol 9: 643515, 2021.
28. Yang WH, Ding CC, Sun T, Rupprecht G, Lin CC, Hsu D and Chi JT: The Hippo pathway effector TAZ regulates ferroptosis in renal cell carcinoma. Cell Rep 28: 2501-2508.e4, 2019.
29. Zhu G, Murshed A, Li H, Ma J, Zhen N, Ding M, Zhu J, Mao S, Tang X, Liu L, *et al*: O-GlcNAcylation enhances sensitivity to RSL3-induced ferroptosis via the YAP/TFRC pathway in liver cancer. Cell Death Discov 7: 83, 2021.
30. Ye S, Xu M, Zhu T, Chen J, Shi S, Jiang H, Zheng Q, Liao Q, Ding X and Xi Y: Cytoglobin promotes sensitivity to ferroptosis by regulating p53-YAP1 axis in colon cancer cells. J Cell Mol Med 25: 3300-3311, 2021.
31. Cao X, Li Y, Wang Y, Yu T, Zhu C, Zhang X and Guan J: Curcumin suppresses tumorigenesis by ferroptosis in breast cancer. PLoS One 17: e0261370, 2022.
32. Livak KJ and Schmittgen TD: Analysis of relative gene expression data using real-time quantitative PCR and the 2(-Delta Delta C(T) method. Methods 25: 402-408, 2001.
33. Stockwell BR, Friedmann Angeli JP, Bayir H, Bush AI, Conrad M, Dixon SJ, Fulda S, Gascón S, Hatzios SK, Kagan VE, *et al*: Ferroptosis: A regulated cell death nexus linking metabolism, redox biology, and disease. Cell 171: 273-285, 2017.
34. Yang WS, SriRamaratnam R, Welsch ME, Shimada K, Skouta R, Viswanathan VS, Cheah JH, Clemons PA, Shamji AF, Clish CB, *et al*: Regulation of ferroptotic cancer cell death by GPX4. Cell 156: 317-331, 2014.
35. Yang Y, Tang H, Zheng J and Yang K: The PER1/HIF-1alpha negative feedback loop promotes ferroptosis and inhibits tumor progression in oral squamous cell carcinoma. Transl Oncol 18: 101360, 2022.
36. Wang R and Zhu G: A narrative review for the Hippo-YAP pathway in cancer survival and immunity: the Yin-Yang dynamics. Transl Cancer Res 11: 262-275, 2022.
37. Tang T, Yang Z, Zhu Q, Wu Y, Sun K, Alahdal M, Zhang Y, Xing Y, Shen Y, Xia T, *et al*: Up-regulation of miR-210 induced by a hypoxic microenvironment promotes breast cancer stem cell metastasis, proliferation, and self-renewal by targeting E-cadherin. FASEB J: Sep 6, 2018 (Epub ahead of print).
38. Marhuenda E, Campillo N, Gabasa M, Martínez-García MA, Campos-Rodríguez F, Gozal D, Navajas D, Alcaraz J, Farré R and Almendros I: Effects of sustained and intermittent hypoxia on human lung cancer cells. Am J Respir Cell Mol Biol 61: 540-544, 2019.
39. Yang L, Zhang W, Wang Y, Zou T, Zhang B, Xu Y, Pang T, Hu Q, Chen M, Wang L, *et al*: Hypoxia-induced miR-214 expression promotes tumour cell proliferation and migration by enhancing the Warburg effect in gastric carcinoma cells. Cancer Lett 414: 44-56, 2018.
40. Pawlus MR and Hu CJ: Enhanceosomes as integrators of hypoxia inducible factor (HIF) and other transcription factors in the hypoxic transcriptional response. Cell Signal 25: 1895-1903, 2013.
41. Jensen RL, Ragel BT, Whang K and Gillespie D: Inhibition of hypoxia inducible factor-1alpha (HIF-1alpha) decreases vascular endothelial growth factor (VEGF) secretion and tumor growth in malignant gliomas. J Neurooncol 78: 233-247, 2006.
42. Forcina GC and Dixon SJ: GPX4 at the crossroads of lipid homeostasis and ferroptosis. Proteomics 19: e1800311, 2019.
43. Xia X, Fan X, Zhao M and Zhu P: The relationship between ferroptosis and tumors: A novel landscape for therapeutic approach. Curr Gene Ther 19: 117-124, 2019.
44. Wang X, Wu M, Zhang X, Li F, Zeng Y, Lin X, Liu X and Liu J: Hypoxia-responsive nanoreactors based on self-enhanced photodynamic sensitization and triggered ferroptosis for cancer synergistic therapy. J Nanobiotechnology 19: 204, 2021.
45. Fan Z, Yang G, Zhang W, Liu Q, Liu G, Liu P, Xu L, Wang J, Yan Z, Han H, *et al*: Hypoxia blocks ferroptosis of hepatocellular carcinoma via suppression of METTL14 triggered YTHDF2-dependent silencing of SLC7A11. J Cell Mol Med 25: 10197-10212, 2021.
46. Wu Y, Wang J, Zhao T, Chen J, Kang L, Wei Y, Han L, Shen L, Long C, Wu S and Wei G: Di-(2-ethylhexyl) phthalate exposure leads to ferroptosis via the HIF-1α/HO-1 signaling pathway in mouse testes. J Hazard Mater 426: 127807, 2022.
47. Shin D, Kim EH, Lee J and Roh JL: Nrf2 inhibition reverses resistance to GPX4 inhibitor-induced ferroptosis in head and neck cancer. Free Radic Biol Med 129: 454-462, 2018.
48. Gong Y, Wang N, Liu N and Dong H: Lipid peroxidation and GPX4 inhibition are common causes for myofibroblast differentiation and ferroptosis. DNA Cell Biol 38: 725-733, 2019.
49. Yamamura S, Goda N, Akizawa H, Kohri N, Balboula AZ, Kobayashi K, Bai H, Takahashi M and Kawahara M: Yes-associated protein 1 translocation through actin cytoskeleton organization in trophectoderm cells. Dev Biol 468: 14-25, 2020.
50. Coelho MA, de Carné Trécesson S, Rana S, Zecchin D, Moore C, Molina-Arcas M, East P, Spencer-Dene B, Nye E, Barnouin K, *et al*: Oncogenic RAS signaling promotes tumor immunoresistance by stabilizing PD-L1 mRNA. Immunity 47: 1083-1099.e6, 2017.
51. Zhou Y, Yang R and Ma G: YAP1 knockdown suppresses the proliferation, migration and invasion of human nasopharyngeal carcinoma cells. Nan Fang Yi Ke Da Xue Xue Bao 39: 286-291, 2019 (In Chinese).